NUMERICAL INVERSION OF THE LAPLACE TRANSFORM FROM THE REAL AXIS

RUBEN G. AIRAPETYAN AND ALEXANDER G. RAMM

Abstract. A numerical method for inversion of the Laplace transform $F(p)$ given for $p > 0$ only is proposed. Recommendations for the choice of the abscissa of convergence and parameters of numerical integration are given. The results of the numerical tests are discussed.

1. Introduction.

The Laplace transform of a function f is:

$$F(p) := \int_0^\infty f(t)e^{-pt}dt, \quad \Re p > 0. \tag{1.1}$$

The inverse formula is well known:

$$f(t) = \frac{1}{2\pi i}\int_{\sigma - i\infty}^{\sigma + i\infty} F(p)e^{pt}dp, \quad \sigma > 0. \tag{1.2}$$

This formula requires knowledge of $F(p)$ on the vertical line $\Re p = \sigma > 0$ of the complex plane. In many applications $F(p)$ is known for $p > 0$ only. The problem is to find $f(t)$ given $F(p)$ for $p > 0$ only.

Much has been written about Laplace transform inversion (see, for example, [1] - [7], [10] - [16], [19], [20], detailed bibliography can be found in [17, 18]). In this note a simple method is proposed for inversion of $F(p)$, $p > 0$. This method is based on the well known analytical inversion formula obtained by means of the Mellin transform ([25]). However, it seems that this method was not studied and not used practically as a numerical inversion method ([6], [14]), [15]).

This method is numerically efficient for the functions $F(p)$ satisfying assumptions stated in Remark 1 and in (3.3): a) the problem is ill-posed and the proposed method often handles ill-posedness better than some standard regularization methods, and b) the relative error of the numerical inversion by the proposed method is considerably

1991 *Mathematics Subject Classification.* Primary: 65R10, 65R30; Secondary: 65E05.

Key words and phrases. Laplace transform, Mellin transform, numerical analytic continuation.

smaller for noisy data, than the error of the standard inversion method (see Sect. 4). In comparison with the methods based on the decomposition into a series of orthogonal polynomials the proposed method in some numerical tests gave lower accuracy for large values of t, however it was in all tests much more stable with respect to a random noise in the data (see results of the numerical tests in Sect. 4).

The idea used in this work is a development of the ideas in [19], [20], [25]. However, there is no discussion of the numerical implementation of this idea in the cited papers. We give such a discussion, an analysis of the numerical algorithm and a description of the results of numerical experiments.

In section 2 the inversion method is outlined. In section 3 a numerical algorithm is discussed. Numerical examples are given in section 4.

2. Outline of the inversion method.

Denote the Mellin transform of F by

$$\hat{F}(s) := M_{p\to s}F(p) := \int_0^\infty F(p)p^{s-1}dp. \tag{2.1}$$

From (1.1) one gets

$$\hat{F}(s) = \Gamma(s)\int_0^\infty f(t)t^{-s}dt, \quad \Gamma(s) := \int_0^\infty e^{-u}u^{s-1}du, \tag{2.2}$$

where $\Gamma(s)$ is the Gamma-function. From (2.2) one gets

$$\hat{f}(1-s) = \frac{\hat{F}(s)}{\Gamma(s)}. \tag{2.3}$$

Therefore

$$\hat{f}(s) := \int_0^\infty f(t)t^{s-1}dt = \frac{\hat{F}(1-s)}{\Gamma(1-s)} = \frac{1}{\Gamma(1-s)}\int_0^\infty F(p)p^{-s}dp. \tag{2.4}$$

To provide convergence at zero for integrals in (2.4) the following condition is assumed:

$$\Re(s) = \sigma \in (0,1). \tag{2.5}$$

The inversion formula for the Mellin transform, applied to (2.3), yields

$$f(t) = \frac{1}{2\pi i}\int_{\sigma-i\infty}^{\sigma+i\infty} \frac{\hat{F}(1-s)}{\Gamma(1-s)}t^{-s}ds. \tag{2.6}$$

It is known (see [8]) that

$$|\Gamma(1-s)| = \sqrt{2\pi}|\xi|^{\frac{1}{2}-\sigma}e^{-\frac{\pi}{2}|\xi|}[1+o(1)] \text{ as } |\xi| \to \infty, \ -\frac{\pi}{2} < \arg(1-s) < \frac{\pi}{2}, \quad (2.7)$$

where $s = \sigma + i\xi$, $\sigma \in (0,1)$, $\xi \in (-\infty, +\infty)$.

Integral (2.6) converges if, for example, for some $a > \frac{\pi}{2}$ one has:

$$\int_{-\infty}^{+\infty} |\hat{F}(1-\sigma-i\xi)|^2 e^{2a|\xi|}d\xi < \infty. \quad (2.8)$$

Remark 1. *As it follows from Lemma 2 in Appendix ($\sigma_0 = 1-\sigma$) that for a fixed $\sigma \in (0,1)$ condition (2.8) holds if $F(p)$ satisfies the following assumptions:*

(i) $F(p)$ admits analytic continuation to the region $|\arg(p)| < a$ for some $a \in (\frac{\pi}{2}, \pi)$;

(ii) $\sup_{|\theta|\le a} \int_0^{+\infty} \left|F(\rho e^{i\theta})\right|^2 \rho^{1-2\sigma}d\rho < \infty$.

The idea of the inversion method based on formula (2.6) consists of using $F(p)$, given for $p > 0$ in formula (2.1), in order to calculate $\hat{F}(s)$ on the line $\Re s = \sigma > 0$.

One of the important applications of the numerical inversion of the Laplace transform from the real axis is related to a problem of the numerical analytic continuation of a function analytic in the complex half-plane $\Re z > 0$, given on the positive semi-axis to complex half-plane $\Re z > 0$. Such numerical analytic continuation is an important step for solving some ill-posed problems of practical interest (see [21]). Assume that $F(p)$ is a Laplace image of some function $f(t)$ such that $F(p)$ can be continued analytically to the half-plane $\Re z > 0$. In order to compute this analytic continuation numerically one can compute Laplace preimage $f(t)$ of $F(p)$ first and then compute the following integral:

$$F(z) = \int_0^\infty e^{-zt}f(t)dt, \quad \Re z > 0. \quad (2.9)$$

A numerical result illustrating this numerical analytic continuation procedure is given in the next section.

3. Numerical implementation of the inversion method.

The proposed inversion method consists of the following steps:

Step 1. Numerical computation of the Mellin transform $\hat{F}(s)$ of a given function $F(p)$.

Fix $\sigma \in (0,1)$, in order to compute $\hat{F}(1-s)$ on a vertical line $\Re(1-s) = 1-\sigma$ rewrite formula (2.1) as:

$$\hat{F}(1-s) = \hat{F}(1-\sigma-i\xi) := \int_0^\infty F(p) p^{-\sigma} e^{-i\xi\log(p)} dp. \tag{3.1}$$

For p approaching zero the integrand in this formula is a rapidly oscillating function. For the numerical computation of $\hat{F}(\sigma+i\xi)$ use a change of variable $p := e^\tau$ and get:

$$\hat{F}(1-s) := \int_{-\infty}^{\infty} F(e^\tau) e^{(1-\sigma)\tau} e^{-i\xi\tau} d\tau$$

$$= \int_0^\infty F(e^\tau) e^{(1-\sigma)\tau} e^{-i\xi\tau} d\tau + \int_0^\infty F(e^{-\tau}) e^{(\sigma-1)\tau} e^{i\xi\tau} d\tau. \tag{3.2}$$

To compute the integrals in (3.2) one can use the Fast Fourier Transform (FFT) and the Inverse Fast Fourier Transform (IFFT). For efficient numerical computation of FFT and IFFT one needs sufficiently rapidly decreasing functions $F(e^\tau)e^{\sigma\tau}$ and $F(e^{-\tau})e^{-\sigma\tau}$. By increasing σ one increases the rate of decay of the function $F(e^{-\tau})e^{-\sigma\tau}$ but decreases the rate of decay of the function $F(e^\tau)e^{\sigma\tau}$. Thus an appropriate choice of σ providing the balance between the decay rates of $F(e^\tau)e^{(1-\sigma)\tau}$ and $F(e^{-\tau})e^{(\sigma-1)\tau}$ is important for this step.

Assume that:

$$|F(p)| \le C_1 p^{-\alpha} \quad \text{for} \quad p \in [1,+\infty), \quad |F(p)| \le C_2 \quad \text{for} \quad p \in [0,1], \tag{3.3}$$

where $\alpha > 0$. Then

$$\left|F(e^\tau)e^{(1-\sigma)\tau}\right| \le C_1 e^{-(\sigma+\alpha-1)\tau}, \quad \left|F(e^{-\tau})e^{(\sigma-1)\tau}\right| \le C_2 e^{-(1-\sigma)\tau}, \quad \text{for} \quad \tau \ge 0.$$

To achieve the balance between the decay rates of $F(e^\tau)e^{(1-\sigma)\tau}$ and $F(e^{-\tau})e^{(\sigma-1)\tau}$ choose σ as the solution to the following equation:

$$\sigma + \alpha - 1 = 1 - \sigma.$$

Thus for $\alpha \in (0,2)$ the optimal choice for σ is the following:

$$\sigma = 1 - \frac{\alpha}{2}. \tag{3.4}$$

If $\alpha \ge 2$, then σ chosen according to (3.4) does not satisfy condition (2.5). In this case one can choose σ to be a small positive number, for example $\sigma = 0.1$.

For numerical integration in (3.2) one has to replace the integration over infinite semiaxes by the integration over finite intervals: $[0,T_1]$ and $[0,T_2]$. For noisy data $\tilde{F}(p) + \delta(p)$ one can choose T_1 and T_2 by the following rules (see [22, pp. 92-94],

[23], [24]). For σ satisfying (2.5) the error generated by noise in the second integral is much less than the error in the first integral in (3.2). Therefore the choice of T_1 is crucial while T_2 can be chosen sufficiently large, because the integrand in the second integral (3.2) decays exponentially..

Assume that $|\delta(p)| \leq \delta_0$ for all nonnegative p. One has the following estimate for the error $\Delta(T_1)$ of the numerical computation of the first integral in (3.2):

$$|\Delta(T_1)| \leq C_1 \int_{T_1}^{\infty} e^{(1-\sigma-\alpha)\tau} d\tau + \int_0^{T_1} \delta_0 e^{(1-\sigma)\tau} d\tau$$

$$\leq \frac{C_1}{\alpha+\sigma-1} e^{-(\alpha+\sigma-1)T_1} + \frac{\delta_0}{1-\sigma}\left(e^{(1-\sigma)T_1} - 1\right). \tag{3.5}$$

Here the term $\frac{C_2\delta_0}{1-\sigma}(1-e^{(\sigma-1)T_2})$ is negligible compared with the second term on the right-hand side of (3.5).

Minimize the right-hand side of (3.5) with respect to T_1 that is choose T_1 solving the following equation:

$$-C_1 e^{-(\alpha+\sigma-1)T_1} + \delta_0 e^{(1-\sigma)T_1} = 0.$$

Hence:

$$T_1 = \frac{1}{\alpha} \log\left(\frac{C_1}{\delta_0}\right). \tag{3.6}$$

For T_1 chosen in (3.6) the computational error generated by the numerical integration in (3.2) is not more than $\Delta_1(\sigma)$, where

$$\Delta_1(\sigma) \leq \frac{\alpha C_1^{\frac{1-\sigma}{\alpha}} \delta_0^{\frac{\alpha+\sigma-1}{\alpha}}}{\alpha+\sigma-1}. \tag{3.7}$$

If $\alpha \in (0,2)$ then for σ chosen in (3.4) and T_1 chosen in (3.6) the computational error generated by the numerical integration in (3.2) is not more than Δ_1, where

$$\Delta_1 \leq \frac{2\sqrt{C_1}\delta_0^{\frac{\alpha}{2}}}{\alpha}. \tag{3.8}$$

Step 2. Numerical computation of the Gamma-function $\Gamma(s)$.

Because the Gamma-function is the Mellin transform of e^{-u} (see (2.2)) to compute $\Gamma(\sigma+i\xi)$ one can use the procedure of Step 1. The error of computation increases for large ξ. Thus for large ξ instead of using (2.2) one can use the following asymptotic formula ([8]):

$$\Gamma(s) = \sqrt{2\pi} e^{-s} e^{(s-\frac{1}{2})\log(s)} \left[1 + \frac{1}{12z} + \frac{1}{288z^2} - \frac{139}{51840z^3} + O\left(\frac{1}{|z|^4}\right)\right]. \tag{3.9}$$

Step 3. Numerical computation of the inverse Mellin transform of $\hat{F}(\sigma+i\xi)/\Gamma(\sigma+i\xi)$.

This step is crucial for the algorithm. First, one has to compute a ratio of two exponentially decreasing functions of ξ and then to compute the inverse Mellin transform. By asymptotic formula (3.9) one can compute the denominator $\Gamma(\sigma+i\xi)$ with high accuracy but even a small noise $\delta(\sigma+i\xi)$ generates the exponentially increasing term $\delta(\sigma+i\xi)/\Gamma(\sigma+i\xi)$, see formula (2.7). Such difficulties reflect the ill-posedness of the inversion of the Laplace transform, they are unavoidable and appear in all of the methods for inversion of the Laplace transform from the real axes. For example in the methods using decomposition of $F(p)$ into the series of orthogonal polynomials one gets rapidly increasing coefficients of this decomposition. For the numerical computation of the inverse Mellin transform (see (2.6)) one has to replace the integration along the infinite line $\Re s=\sigma$ by the numerical integration along the finite interval $\Re s=\sigma$, $|\Im s|\le R$. The numerical efficiency of the proposed algorithm depends crucially on the choice of R. This number R can not be chosen too large, otherwise the ratio $\delta(\sigma+i\xi)/\Gamma(\sigma+i\xi)$ grows. On the other hand R has to be chosen sufficiently large in order to provide a good approximation for integral (2.6). We propose an optimal choice of R.

From (2.6) one gets:

$$f(t)=\frac{t^{-\sigma}}{2\pi i}\left(\int\limits_0^{+i\infty}\frac{\hat{F}(1-\sigma-i\xi)}{\Gamma(1-\sigma-i\xi)}t^{-i\xi}ds+\int\limits_0^{+\infty}\frac{\hat{F}(1-\sigma+i\xi)}{\Gamma(1-\sigma+i\xi)}t^{i\xi}d\xi\right). \tag{3.10}$$

Thus

$$f(t)=\frac{t^{-\sigma}}{2\pi}\int\limits_0^R\Re\left(\frac{\hat{F}(1-\sigma-i\xi)}{\Gamma(1-\sigma-i\xi)}e^{-i\xi\log(t)}\right)d\xi+J(t,R), \tag{3.11}$$

and

$$|J(t,R)|\le\frac{t^{-\sigma}}{2\pi}\int\limits_R^{+\infty}\left|\frac{\hat{F}(1-\sigma-i\xi)}{\Gamma(1-\sigma-i\xi)}\right|d\xi. \tag{3.12}$$

If $\hat{F}(1-\sigma-i\xi)$ is computed on $[0,R]$ with an error, which, by absolute value, does not exceed $\Delta_1(\sigma)$ (see 3.7), then for $f(t)$ computed by the formula

$$f(t)\approx\frac{t^{-\sigma}}{2\pi}\int\limits_0^R\Re\left(\frac{\hat{F}(1-\sigma-i\xi)}{\Gamma(1-\sigma-i\xi)}e^{-i\xi\log(t)}\right)d\xi, \tag{3.13}$$

the computational error is less than $\Delta(t,R)$, where

$$\Delta(t,R) = \frac{t^{-\sigma}}{2\pi}\left(\int_R^{+\infty}\left|\frac{\hat{F}(1-\sigma-i\xi)}{\Gamma(1-\sigma-i\xi)}\right|d\xi + \Delta_1(\sigma)\int_0^R \frac{1}{|\Gamma(1-\sigma-i\xi)|}d\xi\right). \tag{3.14}$$

Minimizing the expression on the right-hand side of the inequality (3.14) with respect to R one gets the optimal value of R as the solution to the following equation:

$$|\hat{F}(1-\sigma-iR)| = \Delta_1(\sigma). \tag{3.15}$$

Since the function $|\hat{F}(1-\sigma-i\xi)|$ is computed at the Step 1, one can use the numerical results of Step 1 to find R.

One can also estimate R in the following way. Integrate both sides of the equation $|\hat{F}(1-\sigma-i\xi)| = \Delta_1(\sigma)$ with respect to ξ on $[R, R+1]$. Then one gets

$$\Delta_1(\sigma) = \int_R^{R+1} |\hat{F}(1-\sigma-i\xi)|d\xi \le \left[\int_R^{R+1} |\hat{F}(1-\sigma-i\xi)|^2 e^{2a\xi}d\xi\right]^{\frac{1}{2}}\left[\int_R^{R+1} e^{-2a\xi}d\xi\right]^{\frac{1}{2}},$$

where a is the same as in Remark 1. Hence one gets:

$$\Delta_1(\sigma) \le e^{-aR}(2a)^{-1/2}(1-e^{-2a})^{-1/2}\mu(R),$$

where

$$\mu(R) = \left[\int_R^{R+1} |\hat{F}(1-\sigma-i\xi)|^2 e^{2a\xi}d\xi\right]^{\frac{1}{2}}.$$

Therefore one has:

$$\log(\Delta_1(\sigma)) \le -aR + \log(\mu(R)) + \frac{1}{2}\log(\frac{1-e^{-2a}}{2a}).$$

Assuming that $\log(\mu(R)) = o(R^{-1})$ for large R, one gets the estimate:

$$R \sim \frac{1}{a}\log([\Delta_1(\sigma)]^{-1}).$$

Remark 2. *Because of the multiplier $t^{-\sigma}$ in formula (3.11) the error $\Delta(t,R)$ increases when t approaches to zero.*

4. Numerical tests.

In order to test the proposed numerical method the function

$$F(p) = \frac{1}{(p+1)^2+1} + \delta_0 r(p) \tag{4.1}$$

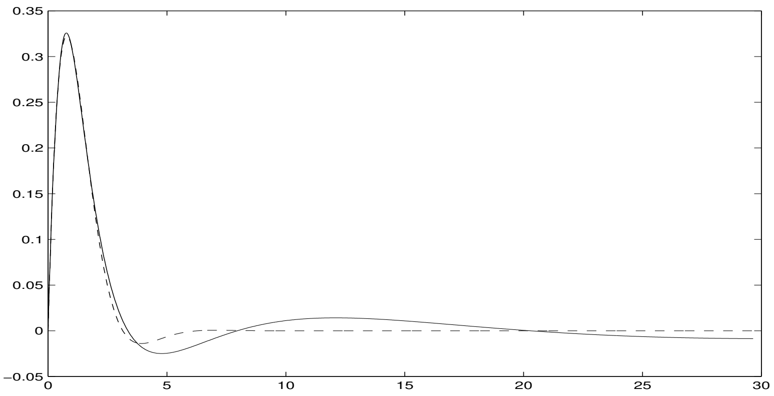

FIGURE 1. $\delta_0 = 10^{-5}$, the solid line corresponds to the graph of $f_{\rm rec}(t)$, the dotted line corresponds to the graph of $f(t)$.

is chosen, where $r(p)$ is a random function taking the values from the interval $[-1,1]$ and δ_0 a parameter characterizing the noise level which is varied in numerical experiments. The chosen function $F(p)$ satisfies assumption (3.3) with $\alpha = 2$ and $C_1 = 1$. Therefore for the Mellin transform the parameters $\sigma = 0.1$ is chosen. For the numerical integration (3.2) and (3.11) parameters T_1 and R are chosen according to formula (3.6 and as an approximate solution to equation (3.15). By using the numerical algorithm described above a function $f_{\rm rec}(t)$ reconstructed from the noisy data has been found. In Figure 1 both $f_{\rm rec}(t)$ and $f(t) = e^{-t}\sin(t)$, which is the exact Laplace preimage of $F(p)$, are plotted.

One can see that for $t > 4$ there is a certain computational error. In Figure 2 the Laplace image $F_r(p)$ of $f_{\rm rec}(t)$ and the function $F(p)$ (left), and $F_r(p) - F(p)$ (right) are plotted.

The graphs show that $F_r(p)$ is close to $F(p)$. Thus the computational error is a result of ill-posedness of the Inverse Laplace Transform from real axis and probably can not be improved without a priori information about the asymptotic behavior for large ξ of $\hat{f}(1-\sigma+i\xi)$, the Mellin transform of $f(t)$.

Figures 3 and 4 show $f_{\rm rec}(t)$ and $f(t) = e^{-t}\sin(t)$ for noise levels $\delta_0 = 10^{-3}$ and $\delta_0 = 10^{-2}$. The accuracy now is lower than for $\delta_0 = 10^{-5}$ but still is satisfactory.

Comparing numerically the proposed method with the numerical methods based on the decomposition into a series of the orthogonal polynomials we have come to the following conclusion. The accuracy of the proposed method is lower than the accuracy of the methods based on the decomposition into a series of orthogonal polynomials if one has precise data or very small perturbation (less than 10^{-14}). However the proposed method is much more stable with respect to perturbations.

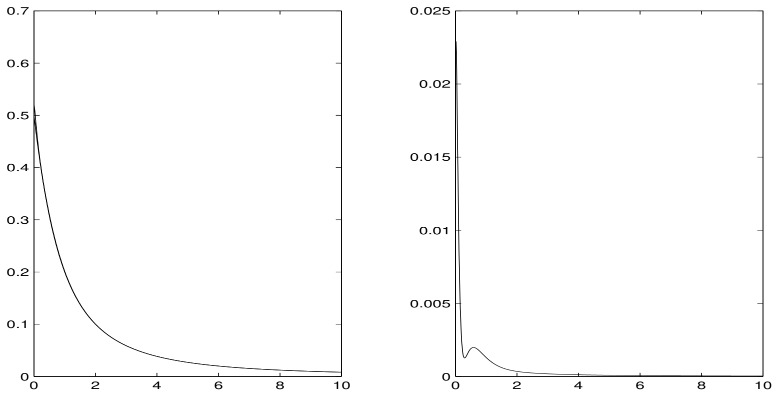

FIGURE 2. $F(p)$ (the dotted line) and $F_r(p)$ (the solid line) are so close that actually can not be separated (left figure), $F_r(p) - F(p)$ (right figure).

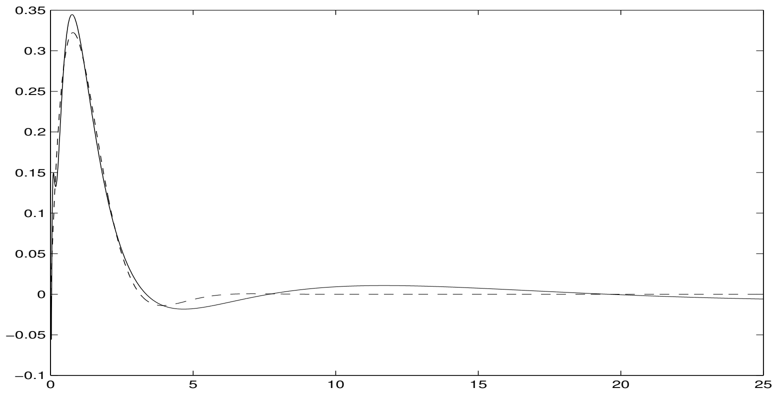

FIGURE 3. $\delta_0 = 10^{-3}$, the solid line corresponds to the graph of $f_{\rm rec}(t)$, the dotted line corresponds to the graph of $f(t)$.

In Figure 5 the results of numerical inversion of Laplace transform by the method based on the decomposition into a series of Legendre polynomials are presented for $\delta_0 = 10^{-13}$.

To compare the proposed numerical method with the numerical method described in [15] the following function is chosen for the next test:

$$F(p) = \frac{1}{(p+1)^2} + \delta_0 r(p). \tag{4.2}$$

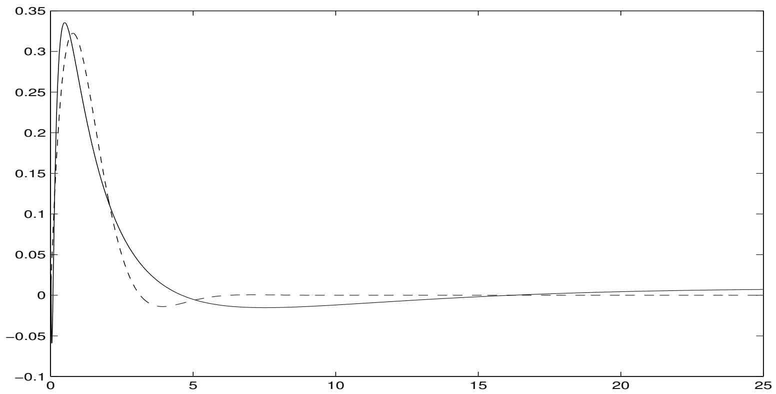

FIGURE 4. $\delta_0 = 10^{-2}$, the solid line corresponds to the graph of $f_{\rm rec}(t)$, the dotted line corresponds to the graph of $f(t)$.

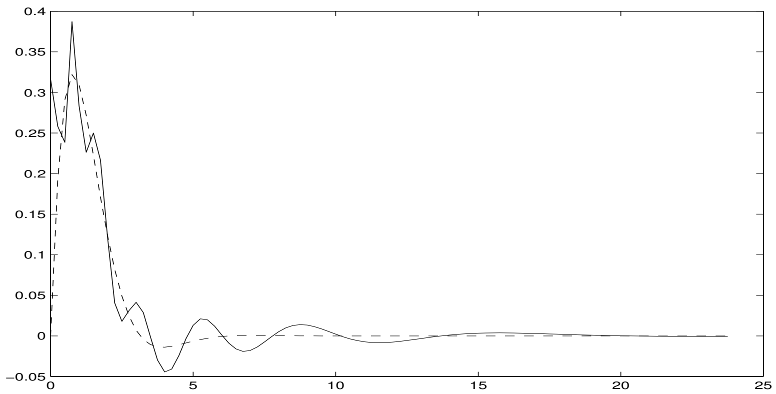

FIGURE 5. $\delta_0 = 10^{-3}$, the solid line corresponds to the graph of $f_{\rm rec}(t)$, the dotted line corresponds to the graph of $f(t)$.

Numerical results are presented in Figures 6 and 7.

The comparison of these numerical results with the results presented in [15, Sect. 5.1] shows that the proposed method is more stable with respect to random noise.

4.1. **Numerical analytical continuation.** The next figures show results of the proposed numerical analytic continuation procedure. For a numerical test the same function (4.1) is chosen with the noise level $\delta_0 = 10^{-5}$.

In Figures 8 and 9 the real and imaginary parts of the functions $F_{\rm num}(z)$ and $F(z)$, continued numerically and analytically are plotted for $\Re z = 0.5$ and $\Re z =$

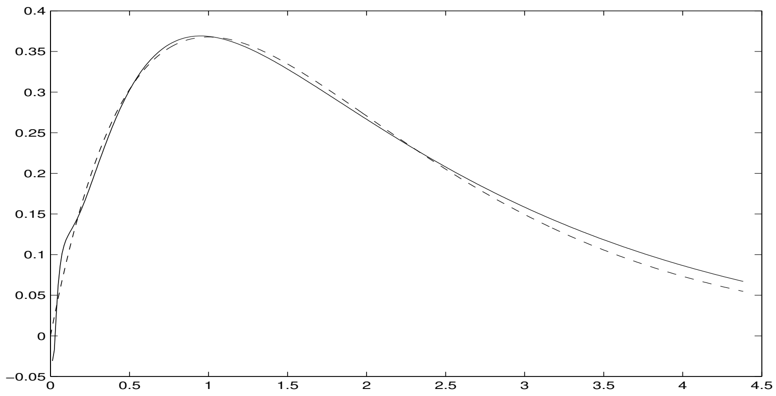

FIGURE 6. $\delta_0 = 10^{-3}$, the solid line corresponds to the graph of $f_{\text{rec}}(t)$, the dotted line corresponds to the graph of $f(t)$.

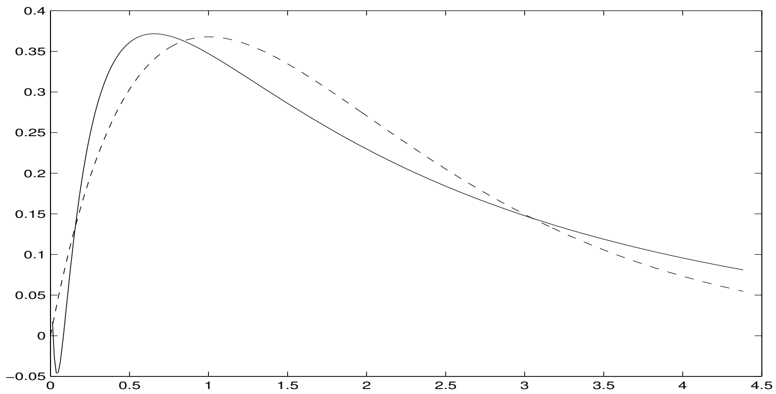

FIGURE 7. $\delta_0 = 10^{-2}$, the solid line corresponds to the graph of $f_{\text{rec}}(t)$, the dotted line corresponds to the graph of $f(t)$.

0.0005, respectively. The accuracy of the numerical analytic continuation to the line $\Re z = 0.0005$ is lower because a pole of the Gamma-function, $z = 0$, is close to the line $\Re z = 0.0005$.

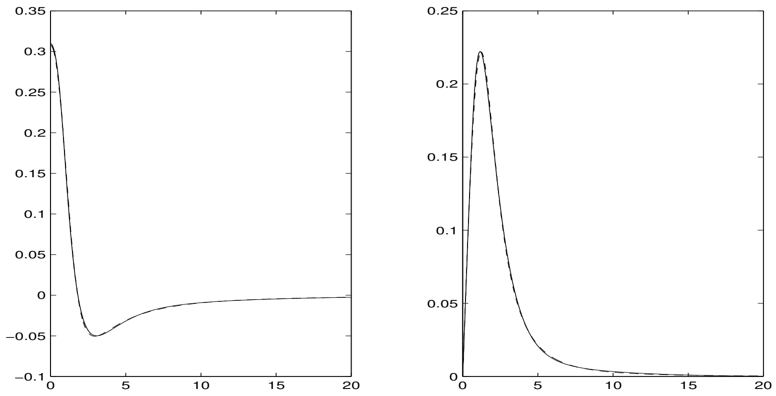

FIGURE 8. $\Re z = 0.5$, the solid line corresponds to the graph of $F_{\text{num}}(z)$, the dotted line corresponds to the graph of $F(z)$, on the left graph the real parts of the functions and on the right graph the imaginary parts of the functions are plotted.

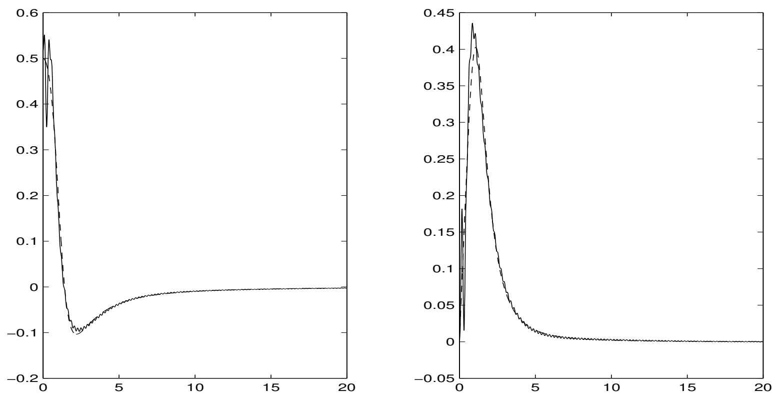

FIGURE 9. $\Re z = 0.0005$

5. APPENDIX

Lemma 1. *Consider the Fourier transform:*

$$\tilde{f}(\xi) = \int_{-\infty}^{+\infty} e^{ix\xi} f(x)\,dx.$$

Let a be a fixed positive number. The function $\tilde{f}(\xi)$ satisfies the condition:

$$\int_{-\infty}^{+\infty} |\tilde{f}(\xi)|^2 e^{2a|\xi|} d\xi < \infty \tag{5.1}$$

if and only if $f(x)$ satisfies the conditions:

(i) $f(x)$ admits analytic continuation to the strip $\{z = x + iy : -\infty < x < +\infty,$ $|y| < a$;

(ii) $\sup_{|y|\le a} \int_{-\infty}^{+\infty} |f(x+iy)|^2 dx < \infty$.

Proof. Let us show first that (i) and (ii) imply (5.1) for $\xi > 0$ (the proof for $\xi < 0$ is similar).

Since $|f(z)|$ is a subharmonic function of $z = x + iy$, $x \in (-\infty, +\infty)$, $|y| < a$, then for $\epsilon > 0$ such that the disc $B_\epsilon(z) := \{w = u + iv : |w - z| \le \epsilon\}$ is a subset of the strip $|v| < a$ one, using the Cauchy inequality, obtains:

$$|f(z)| \le \frac{1}{\pi\epsilon^2} \int_{B_\epsilon(z)} |f(w)| du dv \le \frac{1}{\pi\epsilon^2} \int_{x-\epsilon}^{x+\epsilon} \int_{y-\epsilon}^{y+\epsilon} |f(u+iv)| du dv$$

$$\le \frac{2}{\pi\epsilon} \left[\int_{y-\epsilon}^{y+\epsilon} dv \int_{x-\epsilon}^{x+\epsilon} |f(u+iv)|^2 du \right]^{\frac{1}{2}} \le \frac{2}{\pi\epsilon} \left[\int_{-a}^{a} dv \int_{x-\epsilon}^{x+\epsilon} |f(u+iv)|^2 du \right]^{\frac{1}{2}}. \tag{5.2}$$

It follows from (ii) that for every $v \in [-a, a]$

$$I(v) := \int_{x-\epsilon}^{x+\epsilon} |f(u+iv)|^2 du \to 0, \quad \text{as} \quad |x| \to \infty, \tag{5.3}$$

and $I(v)$ is uniformly bounded:

$$|I(v)| \le \sup_{|v|\le a} \int_{-\infty}^{+\infty} |f(u+iv)|^2 du. \tag{5.4}$$

By Lebesgue's dominated convergence theorem one can pass to the limit, in the integral in (5.2), as $|x| \to +\infty$, and obtain:

$$\sup_{|y|\le a_1 < a} |f(x+iy)| = o(1) \quad \text{for} \quad |x| \to +\infty. \tag{5.5}$$

Fix $y \in (0,a)$. It follows from assumption (i) that

$$\int_{-N}^{N} f(x)e^{ix\xi}dx = \int_{-N}^{N} f(x+iy)e^{i(x+iy)\xi}dx + \int_{0}^{y} f(-N+iy)e^{i(-N+iy)\xi}dy$$

$$-\int_{0}^{y} f(N+iy)e^{i(N+iy)\xi}dy. \tag{5.6}$$

It follows from (5.5) that the last integral in (5.6) tends to zero as $N \to +\infty$. Therefore one gets:

$$e^{y\xi}\tilde{f}(\xi) = \int_{-\infty}^{+\infty} f(x+iy)e^{ix\xi}dx. \tag{5.7}$$

From the Parseval equality one gets:

$$\frac{1}{2\pi}\int_{-\infty}^{+\infty} |\tilde{f}(\xi)|^2 e^{2y\xi}d\xi = \int_{-\infty}^{+\infty} |f(x+iy)|^2 dx. \tag{5.8}$$

Similar argument proves (5.8) with $-a < y \leq 0$.

Therefore one gets:

$$\frac{1}{2\pi}\int_{-\infty}^{+\infty} |\tilde{f}(\xi)|^2 e^{2a|\xi|}d\xi = \sup_{y\in[0,a]}\int_{-\infty}^{+\infty} |f(x+iy)|^2 dx. \tag{5.9}$$

Thus (ii) and (5.9) imply (5.1).

Let us show that (5.1) implies (i-ii). From the inversion formula for the Fourier transform one has:

$$f(x) = \frac{1}{2\pi}\int_{-\infty}^{+\infty} \tilde{f}(\xi)e^{-ix\xi}d\xi. \tag{5.10}$$

For $|y| < a$ define:

$$f(x+iy) := \frac{1}{2\pi}\int_{-\infty}^{+\infty} \tilde{f}(\xi)e^{i(x+iy)\xi}d\xi. \tag{5.11}$$

For any $a_1 \in (-a, a)$ integral on the right-hand side of (5.11) is uniformly majorized by the integral:

$$\frac{1}{2\pi}\int_{-\infty}^{+\infty}|\tilde{f}(\xi)|e^{a_1|\xi|}d\xi \le \frac{1}{2\pi}\left[\int_{-\infty}^{+\infty}|\tilde{f}(\xi)|^2 e^{2a|\xi|}d\xi\right]^{\frac{1}{2}}\left[\int_{-\infty}^{+\infty}e^{-2(a-a_1)|\xi|}d\xi\right]^{\frac{1}{2}}. \tag{5.12}$$

Hence $f(z)$ defined by (5.11) is analytic in the strip $|y| < a$. Condition (ii) follows from (5.1) and (5.9).

Lemma 2. *Consider the Mellin transform (2.1) with* $\Re(s) = \sigma_0 \in (0, 1)$ *and let* $a \in (0, \pi)$ *be a fixed positive number. The function* $\hat{F}(s)$ *satisfies the condition:*

$$\int_{-\infty}^{+\infty}|\hat{F}(\sigma_0 + i\xi)|^2 e^{2a|\xi|}d\xi < \infty \tag{5.13}$$

if and only if $F(p)$ *satisfies the conditions:*

(i) $F(p)$ *admits analytic continuation to the region* $|\arg(p)| < a$*;*

(ii) $\sup_{|\theta|\le a} \int_0^{+\infty} \left|F(\rho e^{i\theta})\right|^2 \rho^{2\sigma_0 - 1}d\rho < \infty.$

Proof. Using the change of variable $p = e^x$, write the Mellin transform (2.1) as the Fourier transform of the function $f(x) := F(e^x)e^{\sigma_0 x}$:

$$\hat{F}(\sigma_0 + i\xi) = \int_{-\infty}^{+\infty} F(e^x)e^{\sigma_0 x}e^{ix\xi}dx.$$

Now Lemma 2 follows from Lemma 1:

Condition (5.13) holds if and only if $F(e^{x+i\theta})e^{\sigma_0(x+i\theta)}$ is analytic in $|\theta| < a$ and

$$\sup_{|\theta|\le a}\int_{-\infty}^{+\infty}|F(e^{x+i\theta})|^2 e^{2\sigma_0 x}dx < \infty.$$

Let $e^x = \rho$ then the above condition is equivalent to

$$\sup_{|\theta|\le a}\int_{0}^{+\infty}|F(\rho e^{i\theta})|^2 \rho^{2\sigma_0 - 1}d\rho < \infty.$$

Acknowledgments

The authors thank referees for useful comments.

References

[1] A. d'Alessio, L. D'Amore, and G. Laccetti, *First results about the Tikhonov regularization methods for numerically inverting a Laplace transform function,* Rend. Accad. Sci. Fis. Mat. Napoli (4), **60** (1993), 75–102.

[2] P. Brianzi and M. Frontini, *On the regularized inversion of the Laplace transform,* Inverse Problems, **7** (1991), 355–368

[3] A. Chakrabarti, *A note on the inversion of Laplace transforms,* Int. J. Math. Educ. Sci. Technol., **21** (1990), 325–328.

[4] D. E. Chauveau, A. C. M. van Rooij, and F. H. Ruymgaart, *Regularized inversion of noisy Laplace transforms,* Adv. in Appl. Math., **15** (1994), 186–201.

[5] C. Cunha and F. Viloche, *An iterative method for the numerical inversion of Laplace transforms,* Math. Comp., **64** (1995), 1193–1198.

[6] B. Davies and B. Martin, *Numerical inversion of the Laplace transform: a survey and comparison of methods*, J. of Comp. Physics, **33** (1979), 1–32.

[7] C.W. Dong, *A regularization method for the numerical inverse of the Laplace transform,* SIAM J. Numer. Anal., **30** (1993), 759–773.

[8] A. Erdélyi, W. Magnus, F. Oberhettinger, and F. G. Tricomi, *Higher Transcendental Functions, Vol. I,* Bateman Manuscript Project, McGraw-Hill, New York, 1954.

[9] G.A. Frolov and M.Y. Kitaev, *Improvement of accuracy in numerical methods for inverting Laplace transforms based on the Post-Widder formula,* Comput. Math. Appl., **36** (1998), 23–34.

[10] G. Giunta, A. Murli, G. Schmid, G. *An analysis of bilinear transform polynomial methods of inversion of Laplace transforms,* Numer. Math., **69** (1995), 269–282.

[11] G. Honig and U. Hirdes, *A method for the numerical inversion of Laplace transforms,* J. Comput. Appl. Math., **10** (1984), 113–132.

[12] M. Iqbal, *On spline regularized inversion of noisy Laplace transforms,* J. Comput. Appl. Math., **83** (1997), 39–54.

[13] D. Jagerman, *An inversion technique for the Laplace transform with application to approximation,* Bell. Syst. Tech. J., **57** (1978), 669-710.

[14] V.I. Krylov and N.S. Skoblya, *Handbook of numerical inversion of the Laplace transform,* (in Russian), Nauka i Technika, Minsk, 1968.

[15] J.G. McWirther and E.R. Pike, *On the numerical inversion of the Laplace transform and similar Fredholm integral equations of the first kind*, J. Phys. A: Math. Gen., **11** (1978),

[16] N.E. Mastorakis, *Numerical inversion of the Laplace transform via fast Fourier transform,* Found. Comput. Decision Sci., **22** (1997), 21–26.

[17] R. Piessens, *A bibliography on numerical inversion of the Laplace transform and applications,* J. Comput. Appl. Math., **1** (1975), 115–128.

[18] R. Piessens and N.D.P. Dang, *A bibliography on numerical inversion of the Laplace transform and applications: a supplement,* J. Comput. Appl. Math., **2** (1976), 225–228.

[19] A.G. Ramm, *Inversion of the Laplace transform from the real axis,* Inverse Problems **2** (1986), L55–L59.

[20] A.G. Ramm, *Multidimensional inverse scattering problems,* Longman/Wiley, New York, 1992, Russian translation of the expanded monograph: (Mir Publishers, Moscow, 1994).

[21] A.G. Ramm, *The ground-penetrating radar problem III,* J. of Inverse and Ill-Posed Problems, 8, N1, (2000), 23-30.

[22] A.G. Ramm, *Random fields estimation theory,* Longman Scientific and Wiley, New York, 1990.

[23] A.G. Ramm, *Stable solutions of some ill-posed problems,* Math. Meth. in Appl. Sci. **3** (1981), 336-363.

[24] A.G. Ramm, *Optimal harmonic synthesis of generalized Fourier series and integrals with randomly perturbed coefficients,* Radiotechnika, **28** (1973), 44-49.
[25] E.T. Titchmarsh, *Introduction to the theory of Fourier integrals*, Oxford Press, 1948.

E-mail address: airapet@math.ksu.edu

E-mail address: ramm@math.ksu.edu

Department of Mathematics, Kansas State University, Manhattan, Kansas 66506, USA